Genes to Cells
平成 27 年 6 月 20 日発刊
第 6 巻、500-511 頁

主論文

Original Article

Disappearance of centroacinar cells in the Notch ligand-deficient pancreas

Short Title: Notch ligands in pancreatic development

Yasuhiro Nakano[1,4], Naoko Negishi[1,6], Seiho Gocho[2], Tetsuya Mine[2], Yuri Sakurai[1], Masaki Yazawa[1], Koichiro Abe[3], Hideo Yagita[6], Sonoko Habu[6], Ryoichiro Kageyama[5], Yoshiya Kawaguchi[4,*], Katsuto Hozumi[1,*]

[1]Department of Immunology and Research Center for Regenerative Medicine, [2]Department of Internal Medicine, [3]Division of Basic Medical Science and Molecular Medicine, Tokai University School of Medicine, 143 Shimokasuya, Isehara, Kanagawa 259-1193, Japan.

[4]Department of Clinical Application, Center for iPS Cell Research and Application, [5]Institute of Virus Research, Kyoto University, 53 Kawahara-cho, Shogoin, Sakyo-ku, Kyoto 606-8507, Japan.

[6]Department of Immunology, Juntendo University School of Medicine, 2-1-1 Hongo, Bunkyo-ku, Tokyo 113-0033, Japan.

*Authors for correspondence: Katsuto Hozumi, phone +81 463 93 1121, FAX +81 463 94 2976, e-mail hozumi@is.icc.u-tokai.ac.jp; Yoshiya Kawaguchi, phone +81 75 366 7049, FAX +81 75 366 7050, e-mail yoshiyak@cira.kyoto-u.ac.jp

Abstract

Notch signaling has been shown to contribute to murine pancreatic development at various stages. Delta-like 1 (Dll1) or Jagged1 (Jag1) are the Notch ligand that solely functions to trigger this signaling during the pancreatic bud stage (~e9.5) or after birth, respectively. However, it has not been elucidated whether these Notch ligands are required at the later stage (e10.5~18.5) when the particular pancreas structures form. Here, we detected the dual expression of Dll1 and Jag1 in the epithelium after e10.5, which was restricted to the ductal-cell lineage, including centroacinar cells expressing Sox9, CD133 and Hes1 but not the ductal-cell markers Hnf1β and DBA, at e18.5. To evaluate the significance of the Notch ligands during this period, we established double-floxed mice of *Dll1* and *Jag1* genes with *Ptf1a-Cre* knock-in allele and examined the effects on development. The abrogation of both ligands but not a single one led to the loss of centroacinar cells, which was due to the decrease in cell proliferation and the increase in cell death, as well as to the reduction of Sox9. These results suggested that Dll1 and Jag1 function redundantly and are necessary to maintain the centroacinar cells as an environmental niche in the developing pancreas.

Introduction

The formation of tissue structures is crucial to obtaining organ functions. The exocrine pancreas is composed of enzyme-producing acini and ductal structures that channel the pancreatic fluid into the duodenum. The exocrine acinus is composed of enzyme-secreting acinar cells and of centroacinar cells located in the center of the acinar structure (Ashizawa *et al.* 2005). The branched ductal tree is sub-divided into the main, interlobular and terminal ducts, the latter of which that connect to the acini (Reichert & Rustgi 2011). Previous studies identified genes involved in the specification and differentiation of acinar and duct cells, but the precise mechanisms underlying the construction of the exocrine pancreatic architecture during the embryonic stages are largely unknown. At approximately embryonic day 9.5 (e9.5) in mice, pancreatogenesis begins with the evagination of endodermal cells from the primitive foregut tube to form the dorsal and ventral pancreatic buds. At first, no obvious ductal structures are observed within the buds, but segregated epithelial cells gradually form the branching ductal tree (Pan & Wright 2011). As development proceeds, at e13.5-15.5, amylase-expressing exocrine acinar cells appear in the "tip" region of the ductal trees, whereas endocrine cells formed in the ductal "trunk" region (Zhou *et al.* 2007). During these stages, lines of acinar cells are observed adjacent to the ductal structures and acinar and centroacinar cells cannot be distinguished by H&E staining. The branching structure of the ducts becomes more complex after that stage, and mature acinar structures are completed at e18.5, when identifiable centroacinar cells appear at the center of the acini.

Previous studies suggested that centroacinar cells function as progenitor cells;

inducible Cre-based cell-tracking experiments showed that Sox9–expressing cells differentiated into all types of pancreatic cells during the embryonic and neonatal stages, including exocrine, endocrine and ductal lineages (Furuyama *et al.* 2011; Kopp *et al.* 2011). Considering their location at the junction of ductal tree and the acini, $Sox9^{+}$ centroacinar cells are thought to be the best candidate for the source of new acinar cell populations at the perinatal stages. Moreover, ALDH1-expressing centroacinar/terminal duct cell populations in adult mouse possess multi-differentiation capacity towards endocrine and exocrine pancreatic cells *in vitro* (Rovira *et al.* 2010). However, the lack of specific markers has prevented the elucidation of how centroacinar cells are formed and maintained in the developing exocrine tissue.

The construction of an acinar structure appears to be associated with the formation of a boundary between acinar cells and the ductal network during pancreatic development. Previous studies showed the pivotal role of Notch signaling in the formation of a boundary between different cell types, such as occurs in the *Drosophila* wing margin and vertebrate somite (Artavanis-Tsakonas *et al.* 1999). Thus, we speculated that Notch signaling is likely involved in the proper construction of exocrine pancreatic tissue, including the acinar structures. Although recent reports demonstrated that Notch signaling functions in controlling endocrine-cell and ductal differentiation in the “trunk” domain (Afelik *et al.* 2012; Horn *et al.* 2012; Shih *et al.* 2012) and that its signaling confines centroacinar cells to the ductal lineage during adulthood (Kopinke *et al.* 2012; Hosokawa *et al.* 2015), the details of how Notch signaling functions in exocrine pancreatic development remains unknown. In this study, we demonstrated that centroacinar cells

comprise the $Sox9^{+}Hnf1\beta^{-}CD133^{+}ALDH1^{+}DBA^{-}$ population that expressed the Notch ligands, Delta-like 1 (Dll1) and Jagged1 (Jag1), as well as Hes1, a target of Notch signaling, at e18.5 in mice. Depleting Dll1 and Jag1 in pancreatic progenitor cells in the Ptf1a-Cre line, in which the recombinase becomes active as early as e10.5, reduced the level of Hes1 expression and caused the loss of centroacinar cells and some of the terminal duct cells at e18.5. These results demonstrated the pivotal role of Dll1/Jag1-mediated Notch signaling in maintaining the centroacinar/terminal duct cells during the construction of the exocrine structure *in vivo*.

Results

The Notch ligands Delta-like1 and Jagged1 are expressed in the developing ductal tree and the centroacinar region during murine pancreatogenesis

As several previous reports showed, the Notch ligands Dll1 and Jag1 exhibited dynamically changing expression patterns during the construction of the pancreatic architecture; Dll1 was expressed in Sox9-expressing epithelial cells in pancreatic buds as early as e9.5, whereas Jag1 expression was not detected at this stage (Fig. 1A,E; Ahnfelt-Rønne *et al.* 2012). From e10.5 to e13.5, almost all of the pancreatic epithelial cells expressed both Dll1 and Jag1 (Fig. 1B,C,F,G; Golson *et al.* 2009a). As cell differentiation and branching of the ductal tree proceeded, different levels of Dll1 expression were detected throughout the Sox9-expressing trunk region and in acinar cells, and Jag1 expression was retained in duct cells but was reduced in acinar cells at e15.5 (Fig. 1D,H; Shih *et al.* 2012). At e18.5, centroacinar cells were identified as the most distal cells with a high N/C ratio in the center of the mature acinar structures (Fig. 1I-M, arrowheads). At this stage, the branching ductal structure was fully developed and could be divided into the following two components based on H&E staining: the main/interlobular and terminal ducts. The former cells were found outside the acini (Fig. 1I-J, thick arrows) and the latter cells were found near the centroacinar cells at the near side of the duct within an acinus (Fig. 1I-J, thin arrows). All of the cells that composed the ductal structures as well as the centroacinar cells expressed Sox9, but we found differential expression of the Notch ligands (Fig. 1I,J,L,M; Table S1 in Supporting information). Dll1 was expressed in the centroacinar regions and a subset of the terminal ducts but not in the interlobular~main

ducts, whereas Jag1 was detected throughout the ductal tree and in the centroacinar cells at e18.5 (Fig. 1I,J,L,M; Table S1 in Supporting information). Thus, the centroacinar cells at this stage expressed both of the Notch ligands and Sox9, whereas the acinar cells expressed neither of the Notch ligands or Sox9. Hes1, the main effector of Notch signaling, was occasionally detected in centroacinar cells, terminal ducts and interlobular~main ducts but not in acinar cells (Fig. 1K; Table S1 in Supporting information), suggesting that a subset of the centroacinar and duct cells received Notch signaling at this stage.

Characterization of the epithelial cells in the centroacinar region at e18.5 in mice

For a more detailed characterization of the centroacinar cells at e18.5, we performed additional immunostaining assays. Our immunofluorescence analyses using two independent antibodies revealed that Hnf1β was expressed in the main/interlobular ducts but that its expression was remarkably reduced in the terminal ducts and was lost in centroacinar cells (Fig. 2A; Table S1 in Supporting information). DBA, a well-known ductal marker, was also expressed strongly in the main/interlobular ducts and weakly in the terminal ducts but not in the centroacinar and acinar cells, thereby having an expression pattern similar to that of Hnf1β at this stage (Fig. 2A,C,D; Fig. S1 and Table S1 in Supporting information). We also detected rare DBA-negative terminal duct cells (Fig. 2C, asterisk; Fig. S1C, green arrows in Supporting information). We found that the expression of CD133, a marker of multipotent progenitors in the developing pancreas *in vitro* (Oshima *et al.* 2007; Immervoll *et al.* 2011), overlapped with that of Sox9 (Fig. 2B; Table S1 in Supporting information) in that both were expressed throughout the ductal tree

and in the centroacinar cells but not in acinar cells. ALDH1, another marker of multipotent progenitors during adulthood (Rovira *et al.* 2010), was restrictively expressed in the centroacinar and terminal ductal regions, and thus the ALDH1-expressing epithelial cells could be divided into two populations, as follows: $Sox9^{+}ALDH1^{+}DBA^{-}$ centroacinar cells (Fig. 2C, arrowhead) and $Sox9^{+}ALDH1^{+}DBA^{+}$ (Fig. 2C, arrows) with rare $Sox9^{+}ALDH1^{+}DBA^{-}$ (Fig. 2C, asterisk) cells in the terminal ductal region (Rovira *et al.* 2010). Taken together, the centroacinar cells could be defined as $Sox9^{+}Hnf1\beta^{-}$ $CD133^{+}ALDH1^{+}DBA^{-}$ with Dll1 and Jag1 expression at e18.5 in mice (Fig. 2E; Table S1 in Supporting information). In contrast, EpCAM was expressed in Sox9-positive duct cells and a few Sox9-negative acinar cells (Fig. 2D), which could be useful at this stage for concentrating amylase-negative epithelial cells in flow cytometric analysis (see below).

Reduced proliferation and accelerated apoptosis accompany reduced Sox9 expression in the Dll1/Jag1-deficient mice

To determine the significance of Notch ligands in the construction of the pancreatic architecture, we first analyzed $Ptf1a^{Cre/+};Dll1^{lox/lox}$ mice and $Ptf1a^{Cre/+};Jag1^{lox/lox}$ mice, in which the Cre-mediated recombination appropriately occurs at e10.5 (Kawaguchi *et al.* 2002; Fujikura *et al.* 2007). In these single knockout mice, no apparent related phenotype of the pancreatic structure was observed during the embryonic stages (Y. Nakano, *et al.* unpublished data), which might be explained by the redundant expression of the Notch ligands from e10.5 to the perinatal stage (Fig. 1). We then analyzed $Ptf1a^{Cre/+};Dll1^{lox/lox};Jag1^{lox/lox}$ doubly deficient mice (Dll1/Jag1 cKO mice). Until

e15.5, we did not observe any related structural phenotype, even when using electron microscopy (Fig. 3A,B, and Fig. S2A,B in Supporting information). Despite no apparent structural defects, we found that the overall level of Sox9 expression was reduced at e15.5 in Dll1/Jag1 cKO mice but not in the single mutant mice (Fig. 3C,D), which is consistent with previous reports that Notch signaling regulates Sox9 expression (Notch-Sox9 axis) (Zong *et al.* 2009; Shih *et al.* 2012). Furthermore, reduced cell proliferation and accelerated apoptosis were observed in the mutants, predominantly in the distal region of the branching ductal tree, including in the primitive acinar structure (Fig. 3E-J). Our PHH3 staining analysis revealed that the cells in the distal ductal epithelium were proliferating more rapidly than those in the proximal ducts from e15.5 to e18.5 in the control mice (Fig. 3E-G). As normal development proceeded, the cell proliferation rate decelerated overall, as reflected by the reduction in the number of $PHH3^+$ cells (e15.5: 298 cells/mm^2, e16.5: 76 cells/mm^2, e17.5: 19 cells/mm^2, e18.5: 20 cells/mm^2; Fig. 3G). In the Dll1/Jag1 cKO mice, the number of $PHH3^+$ cells was significantly lower than that of control mice in both the distal and proximal ducts at all of the stages evaluated (e15.5: 169 cells/mm^2, e16.5: 33 cells/mm^2, e17.5: 7.5 cells/mm^2, e18.5: 2.5 cells/mm^2; Fig. 3G). In addition, we observed accelerated apoptosis, predominantly in the distal region of the ductal tree, in the Dll1/Jag1 cKO mice after e16.5 (Fig. 3H-J). Consistent with this finding, the expression of anti-apoptotic genes, such as *Bcl2* and *Bcl2a*, was significantly down-regulated in the pancreata of the Dll1/Jag1 cKO mice (Fig. S3 in Supporting information). These results demonstrate that Dll1/Jag1-mediated Notch signaling supports the proliferation and survival of cells in the distal portion of the branching ducts,

presumably via the Notch-Sox9 axis.

Loss of centroacinar cells and abrogated acinar construction in Dll1/Jag1-deficient pancreas

Reduced proliferation and accelerated cell death in the distal region of the branching tree (Fig. 3) resulted in abrogated acinar construction in the Dll1/Jag1 cKO mice at e18.5 (Fig. 4A,B). In the primitive acinar structure at e15.5, the amylase-expressing acinar cells were aligned (blue in Fig. 4C,D) but left a vacant space in the center of the primitive acini, which contained Hnf1β-expressing cells (red in Fig. 4C,D) in linear pattern contiguous to the primitive acinar structures in either the control or the Dll1/Jag1 mutant pancreata. It should be noted that Hnf1β^{-}amylase^{-} cells existed within the primitive acinar structures (arrowhead in Fig. 4C,D) and that they also expressed Sox9, Dll1 and Jag1 (arrowhead in Fig. 3C; Fig. S4 in Supporting information). Hes1 expression was detected in a subset of amylase-negative cells regardless of the status of Hnf1β expression in the control mice but was not detected in the Dll1/Jag1 cKO mice (Fig. 4C,D), indicating that Hnf1β^{-}amylase^{-} cells in the primitive acinar structures of the control mice receive Notch signaling. In fact, PHH3^{+} cells were observed among the Hnf1β^{-}amylase^{-} cells in the primitive acinar structures of the control mice, but they were sparse in the Dll1/Jag1 cKO mice (Fig. 4E,F).

During the normal construction of the acinar structures (e15.5-e17.5, Fig. 4G,I,K), the vacant spaces were gradually occupied, and very few vacant spaces were detected in the mature acini of the control mice at e18.5 (Fig. 4A; Fig. S2C,D in

Supporting information). However, in the Dll1/Jag1 cKO mice, the Hnf1β^{-}amylase^{-} cells gradually disappeared (Fig. 4H,J,L) and vacant spaces still existed at e18.5 (Fig. 4B; Fig. S2E,F in Supporting information). In addition to the reduction of Sox9 expression, a similar defect was also observed in the Hes1-deficient pancreas at e17.5 (Fig. S5 in Supporting information). Because the acinar cells were normal in shape and size, with the nucleus localized on the basal side (Fig. 4A,B; Fig. S2C-F in Supporting information), we speculated that the abrogated acinar structures in the Dll1/Jag1 cKO mice was due to the loss of a certain cellular population, most likely the Hnf1β^{-}amylase^{-} cells, in the centroacinar region, rather than the shrinkage or disorganized localization of acinar cells.

To test this hypothesis, we performed additional immunostaining and flow cytometric analyses using the pancreata of e18.5 mice (Fig. 5). We found that, while ALDH1^{-}DBA^{+} main/interlobular duct cells (see Fig. 2C,E) had been preserved, ALDH1^{+}DBA^{-} centroacinar/terminal duct cells (see Fig. 2C,E) were lost in the Dll1/Jag1 cKO mice (Fig. 5A,B). In fact, flow cytometry analyses showed that ALDH1^{+}DBA^{-} cells, which were identified as an Aldefluor^{+}DBA^{-} population (Rovira *et al.* 2010), accounted for 11.3% of the EpCAM-positive epithelial cells in the control mice, whereas this population was markedly decreased to 1.6% in the mutants (Fig. 5E,F,H). Furthermore, we found that CD133-expressing cells co-expressing ALDH1 in the centroacinar/terminal duct region of the control mice (Fig. 5C) were absent in the mutant mice (Fig. 5D). Consistently, another set of flow cytometry showed that the CD133^{+}DBA$^{-/low}$ population was reduced to 3.7% of the EpCAM-positive contingent in the mutant mice, whereas this cells accounted for 33.6% of that contingent in the control mice (Fig. 5E,G,I). Notably, cytospin analysis

showed that the sorted $CD133^{+}DBA^{-/low}$ cells expressed Sox9 but not Hnf1β or amylase (Fig. S6A-O in Supporting information), indicating that the lost cell types in the mutant acinar structures were $Hnf1\beta^{-}amylase^{-}$ cells. It was reported that Aldefluor-positive centroacinar/terminal ductal populations of adult mice exhibit multi-differentiation ability *in vitro* (Rovira *et al.* 2010), thus we next questioned whether the cell population that was lost in the mutants at e18.5 possess a similar ability as adult Aldefluor-positive cells. We found that the sorted $CD133^{+}DBA^{-/low}$ cells from the e18.5 control mice were capable of forming cell sphere and then differentiating into both endocrine and exocrine lineages (Fig. S6P-S in Supporting Information). From these findings, we concluded that the lost cell types in Dll1/Jag1 cKO mice, which were identified as $Hnf1\beta^{-}amylase^{-}$, $ALDH1^{+}DBA^{-}$ or $CD133^{+}DBA^{-/low}$ cells in the control mice, are centroacinar and a part of terminal duct cells that share a differentiation capacity that is similar to that of adult $Aldefluor^{+}$ cells.

Dilated ducts in Dll1/Jag1-deficient pancreas

In addition to the disappearance of centroacinar/terminal duct cells, we observed that the lumens of the main/interlobular ducts were dilated. As early as e18.5, some of DBA-positive duct cells had an abnormal cuboidal shape, 66% of the duct cells lacked CD133 and the ductal lumens were dilated in the mutant mice (Fig. 4B,5D). The mutant phenotypes, including the hypoplastic pancreas, the loss of centroacinar/terminal duct cells and ductal dilatation were progressive at e18.5 (Fig. 5) and were more severe at P3 (Fig. S7 in Supporting information).

Discussion

The dynamically changing patterns of expression of the Notch-related genes during the construction of the exocrine pancreatic architecture suggested that the strength of Notch signaling is spatiotemporally determined in the developing pancreas, thereby regionally controlling cell differentiation and the development of tissue structures. Consistent with this hypothesis, modulating the expression of Notch-related genes produced different phenotypes, depending on the timing of gene activation or inactivation. Thus, interpreting each experimental result requires careful attention. For example, the conditional depletion of Mib1, which is indispensable for the endocytosis of Notch ligands to trigger Notch signaling, beginning at the anterior definitive endoderm stage (e7.5~) in a FoxA2-Cre line lead to the reduction and complete disappearance of the progenitor cells in trunk region at e12.5 and e15.5 (Horn *et al.* 2012), respectively, whereas the number of these cells were the same at e13.5 as at e12.5 and were slightly reduced at e15.5 in the Dll1/Jag1 cKO mice produced using the Ptf1a-Cre line compared to the control mice (Y. Nakano, *et al.* unpublished data). These results suggested that the trunk/tip patterning of the ductal tree was not severely impaired depleting Dll1/Jag1-mediated Notch signaling as early as e10.5. Although the strong expression of Dll1 and Jag1 and the high incidence of Hes1-positive cells at the later developmental stages indicated that Notch activity remained strong in the tip region, including in the centroacinar/terminal duct cells, Notch signaling appeared to be negatively regulated in the acinar cells; no Hes1-expressing cells were detected at this stage and the Notch inhibitor Numb/Numb1 was preferentially observed in acinar cells (Yoshida *et al.* 2003). Thus, the formation of a boundary between

the Notch-active and -inactive cell types potentially plays a pivotal role in the determination of the distal ductal and acinar cell fates, thereby maintaining the acinar structures. Based on this hypothesis, we focused on the centroacinar cells located at the junction between the acinar and ductal structures. In this study, we believe that we have provided the first evidence supporting the indispensable role of the Notch ligands in the maintenance of centroacinar cells and acinar structures.

The lack of specific markers has prevented us from elucidating how centroacinar cells are formed and maintained and how the acinar structures are constructed during embryogenesis; however, we defined the centroacinar cells as the $Sox9^{+}Hnf1\beta^{-}$ $CD133^{+}ALDH1^{+}DBA^{-}$ cells expressing the Notch ligands Dll1 and Jag1 at e18.5 and demonstrated that these cells were lost in Dll1/Jag1 cKO mice. We found that the $Hnf1\beta^{-}Amylase^{-}$ epithelial cells in primitive acinar structures at e15.5, during the construction of acinar structures, were highly proliferative. Notably, they frequently exhibited the expression of Hes1, a typical target of Notch signaling. In the Dll1/Jag1 cKO mice at e15.5, we detected a considerable number of $Hnf1\beta^{-}amylase^{-}$ cells, suggesting that the formation of primitive acinar structures could be initiated in the absence of the Notch ligands. However, the $Hnf1\beta^{-}amylase^{-}$ cells did not proliferate efficiently and were eliminated through apoptosis, leading to abrogated acinar structures associated with the loss of centroacinar cells in the mutant mice. Although the lack of specific cell markers makes it currently impossible to precisely trace the fate of the $Hnf1\beta^{-}amylase^{-}$ cells, we speculated that this cell population is the best candidate for the centroacinar/terminal ductal cell progenitors.

We showed that the expression of Sox9 was reduced in the Notch ligand-deficient mice, which was consistent with the results of a previous report concerning the Notch-Sox9 axis (Shih *et al.* 2012). Although this has not been clearly delineated, the acinar structures of the Sox9-depleted mutant obtained using the Pdx1-Cre line, in which genetic deletion is mediated by Cre recombinase driven by the Pdx1 promoter, appeared very similar to those of the Dll1/Jag1 cKO mice or the Hes1-deficient mice, in which vacant spaces remained at e18.5 (Seymour *et al.* 2007). Considering that the expression of the Notch ligands remained strong in the centroacinar cells, one may naturally assume that the activated Notch-Sox9 axis in this region, particularly that of the Hnf1β^{-}amylase^{-} cells, functions in proper acinar construction and the maintenance of centroacinar cells. In addition, another mutant phenotype of the Dll1/Jag1 cKO mice was the progressive dilatation of the main/interlobular ducts. This condition was detected at e18.5 and was more severe at P3. The inducible Cre-mediated Sox9 knockout caused defects in the formation of ductal-cell cilia (Shih *et al.* 2012), resulting in a dilated ductal phenotype similar to that found in the current study. Thus, the reduction of Sox9 expression is also likely the key mechanism underlying the ductal-dilatation phenotype in the Dll1/Jag1 cKO mice.

Experimental procedures

Mice

The protocol for generating mice bearing a floxed allele of *Dll1* (*Dll1*^{lox}) or *Jag1* (*Jag1*^{lox}) was described previously (Hozumi *et al.* 2004; Brooker *et al.* 2006). To obtain the conditional deletion of the *Dll1* and/or *Jag1* genes within the pancreatic epithelial cells, we used *Ptf1a-Cre* knock-in mice (Kawaguchi *et al.* 2002). The expression of neither Dll1 and Jag1 was detected in the developing pancreas of the Dll1/Jag1 cKO mice, resulting in the disappearance of the cleaved fragments of Notch receptors. Mice lacking the *Ptf1a-Cre allele* were used as controls for the *Notch ligand* cKO mice, except in the experiment in which X-gal staining was used to monitor gene deletion by the cre recombinase encoded by the CAG-CAT-lacZ transgene (Araki *et al.* 1995). The generation of the *Hes1* heterozygote mice was described previously (Ishibashi *et al.* 1995), and these mice were inbred to obtain knockout embryos (Fukuda *et al.* 2006). All of the mice were maintained in specific pathogen-free conditions, and all of the mouse experiments were approved by the university's Animal Experimentation Committee (Tokai University, Kanagawa, Japan).

Immunolabeling and statistical analysis

Immunolabeling was performed as previously described (Furuyama *et al.* 2011). Briefly, dissected tissues were fixed using ice-cold 4% paraformaldehyde, paraffin-embedded and cut into 2- to 3-μm-thick sections. Immunolabeling was conducted using the primary antibodies listed in Table S2 in Supporting information. For immunofluorescent staining,

the bound antibodies were visualized using fluorescent secondary antibodies (Table S3 in Supporting information), and the samples were examined using fluorescence microscopy (BZ-9000, Keyence). TUNEL staining (Promega) was performed according to the manufacturer's instructions. To estimate the frequency of PHH3- or TUNEL-positive cells in the pancreatic epithelium, whole pancreatic tissues obtained from embryos were cut into 2-μm-thick serial sections, the $PHH3^+$ or $TUNEL^+$ cells were counted, and their ratios to all of the epithelial cells was calculated for every section. The data were expressed as the mean values ± SD.

Flow cytometry

The PE-conjugated anti-CD133 antibody and biotinylated-DBA lectin were purchased from eBioscience and Vector, respectively. APC-conjugated anti-EpCAM antibodies were purchased from BioLegend. The Aldefluor Kit (StemCell Technologies) was used according to the manufacturer's instructions. Pancreatic buds obtained from e18.5 embryos were dissociated using 0.05% trypsin/0.53 mM EDTA (Wako) for 20 minutes at 37°C and were triturated gently using a pipette. Single-cell suspensions were incubated with several antibodies for 15 minutes on ice. After washing, flow cytometric analysis and sorting were conducted using a FACSCalibur system and a FACSAria system, respectively (BD Biosciences).

Acknowledgements

We are grateful to T. Sudo and J. Miyazaki for the generous gifts of the anti-Hes1 antibody

and the CAG-CAT-lacZ mice and to M. Tsujimoto, A. Fukuda, K. Hirano, A. Sakai, M. Tanigawa, K. Ishikawa, Y. Okada, N. Kawabe, T. Saso, K. Okamoto-Furuta, H. Kohda, K. Tokunaga, T. Shirao and K. Mitsunaga for their technical assistance. We also thank Y. Inagaki, K. Furuyama and T. Masui for helpful discussions.

Author Contributions

YN, YK and KH conceived the concept and design of the study; YN, NN, SG, YS, MY, KA and KH performed the experiments and acquired the data; KA, HY and RK provided materials; TM and SH contributed to supervising the study; and YK and KH wrote the manuscript, with contributions from all of the authors.

References

Afelik, S., Qu, X., Hasrouni, E., Bukys, M.A., Deering, T., Nieuwoudt, S., Rogers, W., Macdonald, R.J. & Jensen, J. (2012) Notch-mediated patterning and cell fate allocation of pancreatic progenitor cells. *Development* **139**, 1744-1753.

Ahnfelt-Rønne, J., Jørgensen, M.C., Klinck, R., Jensen, J.N., Füchtbauer, E.M., Deering, T., MacDonald, R.J., Wright, C.V., Madsen, O.D. & Serup, P. (2012) Ptf1a-mediated control of Dll1 reveals an alternative to the lateral inhibition mechanism. *Development* **139**, 33-45.

Araki, K., Araki, M., Miyazaki, J. & Vassalli, P. (1995) Site-specific recombination of a transgene in fertilized eggs by transient expression of Cre recombinase. *Proc Natl Acad Sci U S A* **92**, 160-164.

Artavanis-Tsakonas, S., Rand, M.D. & Lake, R.J. (1999) Notch signaling: cell fate control and signal integration in development. *Science* **284**, 770-776.

Ashizawa, N., Sakai, T., Yoneyama, T., Naora, H. & Kinoshita, Y. (2005) Three-dimensional structure of peripheral exocrine gland in rat pancreas: reconstruction using transmission electron microscopic examination of serial sections. *Pancreas* **31**, 401-404.

Brooker, R., Hozumi, K. & Lewis, J. (2006) Notch ligands with contrasting functions: Jagged1 and Delta1 in the mouse inner ear. *Development* **133**, 1277-1286.

Fujikura, J., Hosoda, K., Kawaguchi, Y. *et al.* (2007) Rbp-j regulates expansion of pancreatic epithelial cells and their differentiation into exocrine cells during mouse development. *Dev Dyn* **236**, 2779-2791.

Fukuda, A., Kawaguchi, Y., Furuyama, K., Kodama, S., Horiguchi, M., Kuhara, T., Koizumi, M., Boyer, D.F., Fujimoto, K., Doi, R., Kageyama, R., Wright, C.V. & Chiba, T. (2006) Ectopic pancreas formation in Hes1 -knockout mice reveals plasticity of endodermal progenitors of the gut, bile duct, and pancreas. *J Clin Invest* **116**, 1484-1493.

Furuyama, K., Kawaguchi, Y., Akiyama, H. *et al.* (2011) Continuous cell supply from a Sox9-expressing progenitor zone in adult liver, exocrine pancreas and intestine. *Nat Genet* **43**, 34-41.

Golson, M.L., Le Lay, J., Gao, N., Brämswig, N., Loomes, K.M., Oakey, R., May, C.L., White, P. & Kaestner, K.H. (2009a) Jagged1 is a competitive inhibitor of Notch signaling in the embryonic pancreas. *Mech Dev* **126**, 687-699.

Golson, M.L., Loomes, K.M., Oakey, R. & Kaestner, K.H. (2009b) Ductal malformation and pancreatitis in mice caused by conditional Jag1 deletion. *Gastroenterology* **136**, 1761-1771.e1761.

Horn, S., Kobberup, S., Jørgensen, M.C., Kalisz, M., Klein, T., Kageyama, R., Gegg, M., Lickert, H., Lindner, J., Magnuson, M.A., Kong, Y.Y., Serup, P., Ahnfelt-Rønne, J. & Jensen, J.N. (2012) Mind bomb 1 is required for pancreatic β-cell formation. *Proc Natl Acad Sci U S A* **109**, 7356-7361.

Hosokawa, S., Furuyama, K., Horiguchi, M., Aoyama, Y., Tsuboi, K., Sakikubo, M., Goto, T., Hirata, K., Tanabe, W., Nakano, Y., Akiyama, H., Kageyama, R., Uemoto, S. & Kawaguchi, Y. (2015) Impact of Sox9 Dosage and Hes1-mediated Notch Signaling in Controlling the Plasticity of Adult Pancreatic Duct Cells in Mice. *Sci Rep* **5**, 8518.

Hozumi, K., Negishi, N., Suzuki, D., Abe, N., Sotomaru, Y., Tamaoki, N., Mailhos, C.,

Ish-Horowicz, D., Habu, S. & Owen, M.J. (2004) Delta-like 1 is necessary for the generation of marginal zone B cells but not T cells in vivo. *Nat Immunol* **5**, 638-644.

Immervoll, H., Hoem, D., Steffensen, O.J., Miletic, H. & Molven, A. (2011) Visualization of CD44 and CD133 in normal pancreas and pancreatic ductal adenocarcinomas: non-overlapping membrane expression in cell populations positive for both markers. *J Histochem Cytochem* **59**, 441-455.

Ishibashi, M., Ang, S.L., Shiota, K., Nakanishi, S., Kageyama, R. & Guillemot, F. (1995) Targeted disruption of mammalian hairy and Enhancer of split homolog-1 (HES-1) leads to up-regulation of neural helix-loop-helix factors, premature neurogenesis, and severe neural tube defects. *Genes Dev* **9**, 3136-3148.

Kawaguchi, Y., Cooper, B., Gannon, M., Ray, M., MacDonald, R.J. & Wright, C.V. (2002) The role of the transcriptional regulator Ptf1a in converting intestinal to pancreatic progenitors. *Nat Genet* **32**, 128-134.

Kopinke, D., Brailsford, M., Pan, F.C., Magnuson, M.A., Wright, C.V. & Murtaugh, L.C. (2012) Ongoing Notch signaling maintains phenotypic fidelity in the adult exocrine pancreas. *Dev Biol* **362**, 57-64.

Kopp, J.L., Dubois, C.L., Schaffer, A.E., Hao, E., Shih, H.P., Seymour, P.A., Ma, J. & Sander, M. (2011) Sox9+ ductal cells are multipotent progenitors throughout development but do not produce new endocrine cells in the normal or injured adult pancreas. *Development* **138**, 653-665.

Oshima, Y., Suzuki, A., Kawashimo, K., Ishikawa, M., Ohkohchi, N. & Taniguchi, H. (2007) Isolation of mouse pancreatic ductal progenitor cells expressing CD133 and c-Met

by flow cytometric cell sorting. *Gastroenterology* **132**, 720-732.

Pan, F.C. & Wright, C. (2011) Pancreas organogenesis: from bud to plexus to gland. *Dev Dyn* **240**, 530-565.

Reichert, M. & Rustgi, A.K. (2011) Pancreatic ductal cells in development, regeneration, and neoplasia. *J Clin Invest* **121**, 4572-4578.

Rovira, M., Scott, S.G., Liss, A.S., Jensen, J., Thayer, S.P. & Leach, S.D. (2010) Isolation and characterization of centroacinar/terminal ductal progenitor cells in adult mouse pancreas. *Proc Natl Acad Sci U S A* **107**, 75-80.

Seymour, P.A., Freude, K.K., Tran, M.N., Mayes, E.E., Jensen, J., Kist, R., Scherer, G. & Sander, M. (2007) SOX9 is required for maintenance of the pancreatic progenitor cell pool. *Proc Natl Acad Sci U S A* **104**, 1865-1870.

Shih, H.P., Kopp, J.L., Sandhu, M., Dubois, C.L., Seymour, P.A., Grapin-Botton, A. & Sander, M. (2012) A Notch-dependent molecular circuitry initiates pancreatic endocrine and ductal cell differentiation. *Development* **139**, 2488-2499.

Yoshida, T., Tokunaga, A., Nakao, K. & Okano, H. (2003) Distinct expression patterns of splicing isoforms of mNumb in the endocrine lineage of developing pancreas. *Differentiation* **71**, 486-495.

Zhou, Q., Law, A.C., Rajagopal, J., Anderson, W.J., Gray, P.A. & Melton, D.A. (2007) A multipotent progenitor domain guides pancreatic organogenesis. *Dev Cell* **13**, 103-114.

Zong, Y., Panikkar, A., Xu, J., Antoniou, A., Raynaud, P., Lemaigre, F. & Stanger, B.Z. (2009) Notch signaling controls liver development by regulating biliary differentiation. *Development* **136**, 1727-1739.

Figure legends

Figure 1. Expression of the Notch ligands and Sox9 during murine pancreatogenesis.

(A-H) Immunofluorescence analysis of pancreatic tissue from e9.5 to e15.5 mice was performed using anti-Dll1 (green; A-D), anti-Jag1 (green; E-H) and anti-Sox9 (red) Abs. The dotted lines indicate the pancreatic or gut epithelium (Panc, Gut) at e9.5 or e10.5, the boundary between the epithelial (Epi) and mesenchymal (Mes) regions at e13.5, and the primitive acinar structures (Aci) and ductal (Du) regions at e15.5. (I-K) The co-expression of Dll1, Jag1 or Hes1 (green) and Sox9 was also observed (red) at e18.5. Centroacinar cells (arrowheads) were identified in the center of the mature acinar structures. The branching ductal structures were fully developed and could be divided into two components, the main/interlobular ducts (MD/ID, thick arrows) and the terminal ducts (thin arrows). The same sections were used for H&E staining (I'-K'). (L, M) Expression of Dll1 and Jag1 (green) in the centroacinar region was confirmed, with the cellular boundary identified through anti-β-catenin staining (blue). Centroacinar cells are indicated by arrowheads. All of the sections were also stained using DAPI. Original magnification, 400x. Bars: 50 μm.

Figure 2. Characterization of the epithelial cells in the centroacinar region.

(A-D) Epithelial cells residing in the centroacinar regions of the fetal pancreas (e18.5) were identified by their expression of various cellular markers: DBA (green in A, C; blue in D), Sox9 (red in A, C, D; green in B), Hnf1β (blue, A), CD133 (red, B), ALDH1 (blue,

C) or EpCAM (green, D). Centroacinar, terminal duct and main/interlobular duct cells are indicated by arrowheads and thin and thick arrows, respectively, as shown in Figure 1. Cells with red staining (Sox9 or CD133) with or without blue staining (Hnf1β or ALDH1) are indicated by purple or white arrowheads/arrows, respectively, and those stained with red and green (Sox9 or EpCAM) stained are indicated by yellow arrowheads/arrows. The asterisk in C indicates DBA-negative terminal duct cells. The expression of ALDH1 was also observed in the main ducts (Main Duct, inset in C). The same sections were used for H&E staining (A'-D'). Original magnification, 400x. Bars: 50 μm. (E) Exocrine tissue was completed and composed of branching duct structure with centroacinar (CA), terminal duct (TD) and main/interlobular duct (MD/ID) cells and acinar cells at e18.5. These cell populations were identified with various cell markers described.

Figure 3. Reduction of Sox9 expression accompanied with the decrease of proliferation and the increase of apoptosis in Dll1/Jag1-deficient pancreas.

(A-D) H&E staining and the expression of Sox9 (green), Hnf1β (red) and amylase (blue) were examined in control (Cont; A, C) and Dll1/Jag1-deficient (Dll1/Jag1 cKO; B, D) pancreatic tissues at e15.5. Arrowhead indicates $Sox9^{+}Hnf1\beta^{-}amylase^{-}$ cell in the primitive acinar structure. (E-G) The cell proliferation status in control (Cont; E) and Dll1/Jag1-deficient (Dll1/Jag1 cKO; F) pancreatic tissues at e15.5 was monitored using PHH3 immunohistochemistry (arrowheads; E, F). The number of $PHH3^{+}$ cells in the epithelial areas (1 mm^2) in sections of the pancreata of e15.5 to e18.5 embryos were counted (G). The values are the mean values± SD (n=3 to 4; *, $P<0.05$; **, $P<0.01$). Dis,

distal region; Pro, proximal region. (H-J) Apototic cells were detected using TUNEL staining in control (Cont; H) and Dll1/Jag1-deficient (Dll1/Jag1 cKO; I) pancreatic tissues at e17.5. The TUNEL$^+$ cells in Dll1/Jag1-deficient tissue are indicated by arrowheads (distal area, I) or thick arrows (proximal area, I). The number of TUNEL$^+$ cells in the epithelial areas (1 mm^2) in the sections of pancreata from e15.5 to e18.5 embryos (J) were counted, as shown in G. Original magnification for all of the images, 400x; bars: 50 μm.

Figure 4. Construction of the acinar structures in Dll1/Jag1-deficient embryos.

(A, B) H&E staining of control (Cont; A) and Dll1/Jag1-deficient (Dll1/Jag1 cKO; B) fetal pancreata at e18.5. (C, D) The expression of Hes1 (green in C and D), Hnf1β (red) and amylase (blue) was examined in control (Cont; C) and Dll1/Jag1-deficient (Dll1/Jag1 cKO; D) pancreata at e15.5. Hnf1β$^-$amylase$^-$ cells that expressed or did not express Hes1 are indicated by green (C) or white (D) arrowheads, respectively. Hnf1β$^+$ cells that expressed or did not express Hes1 are also indicated by yellow (C) or red (D), respectively. The same sections were used for H&E staining (C', D'). (E, F) PHH3 was also detected with Hnf1β and amylase as shown in C and D. PHH3$^+$Hnf1β$^-$amylase$^-$ cells were depicted by white arrowheads. (G-L) Immunofluorescence analysis of pancreatic tissues from e15.5 to e17.5 mice was performed using anti-amylase (green) and anti-Hnf1β Abs. Hnf1β$^-$ Amylase$^-$ cells were represented by arrowheads. Hnf1β$^+$ cells connected to the cell layer of amylase-expressing cells (green) were depicted by arrows. The same sections were used for H&E staining (G'-L'). Original magnification of all of the images, 400x; bar: 50 μm.

Figure 5. Loss of centroacinar/terminal duct cells in the Dll1/Jag1-deficient pancreas. (A-D) Immunofluorescence analysis of the expression of DBA (green in A and B, red in C and D) and ALDH1 (red in A and B) or CD133 (green in C and D) in control (Cont; A, C) or Dll1/Jag1-deficient (Dll1/Jag1 cKO; B, D) pancreata from e18.5 embryos was performed. Arrowheads, thick and thin arrows indicate centroacinar, terminal duct and main/interlobular duct cells, respectively, as shown in Figures 1 and 2. Intact ducts ($CD133^+DBA^+$) were observed in the double-deficient pancreas (inset in H). The asterisks indicate the loss of centroacinar cells; the cross indicates an enlarged ductal lumen in a Dll1/Jag1-deficient pancreas. The same sections were used for H&E staining (A'-D'). Original magnification, 400x. Bars: 50 μm. (E-G) The cells of fetal pancreata from e18.5 control (Cont) and Dll1/Jag1-deficient (Dll1/Jag1 cKO) embryos were dissociated, and single-cell suspensions were prepared. The cells were stained using a DBA (F, G), Aldefluor (F) or an anti-CD133 mAb (G) and an anti-EpCAM mAb (E) and were analyzed using flow cytometry. To determine the population negative for ALDH activity, the relevant profiles (upper panels) were compared with those representing control staining with a specific inhibitor of ALDH, DEAB (lower panels), and the boundaries were adjusted according to the frequencies of the $Aldefluor^+$ populations that were provided with the inhibitor, which were fewer than 1% (F). The immature epithelial cells of the e18.5 pancreas could be enriched using EpCAM-positive gating in the assay (E). The numbers in the plots represent the frequency of cells lying in the indicated regions within the gate (n=5, % ± SD). (H, I) The absolute number of cells in the indicated fractions of $EpCAM^+$ cells from the control (Cont) and Dll1/Jag1-deficient (D1/J1cKO) e18.5

embryos were calculated (n=5, mean ± SD). CA, centroacinar cells; TD, terminal duct cells; MD/ID, main/interlobular duct cells. ***indicate differences determined using unpaired Student's *t*-test at P<0.001.

Nakano Fig.1

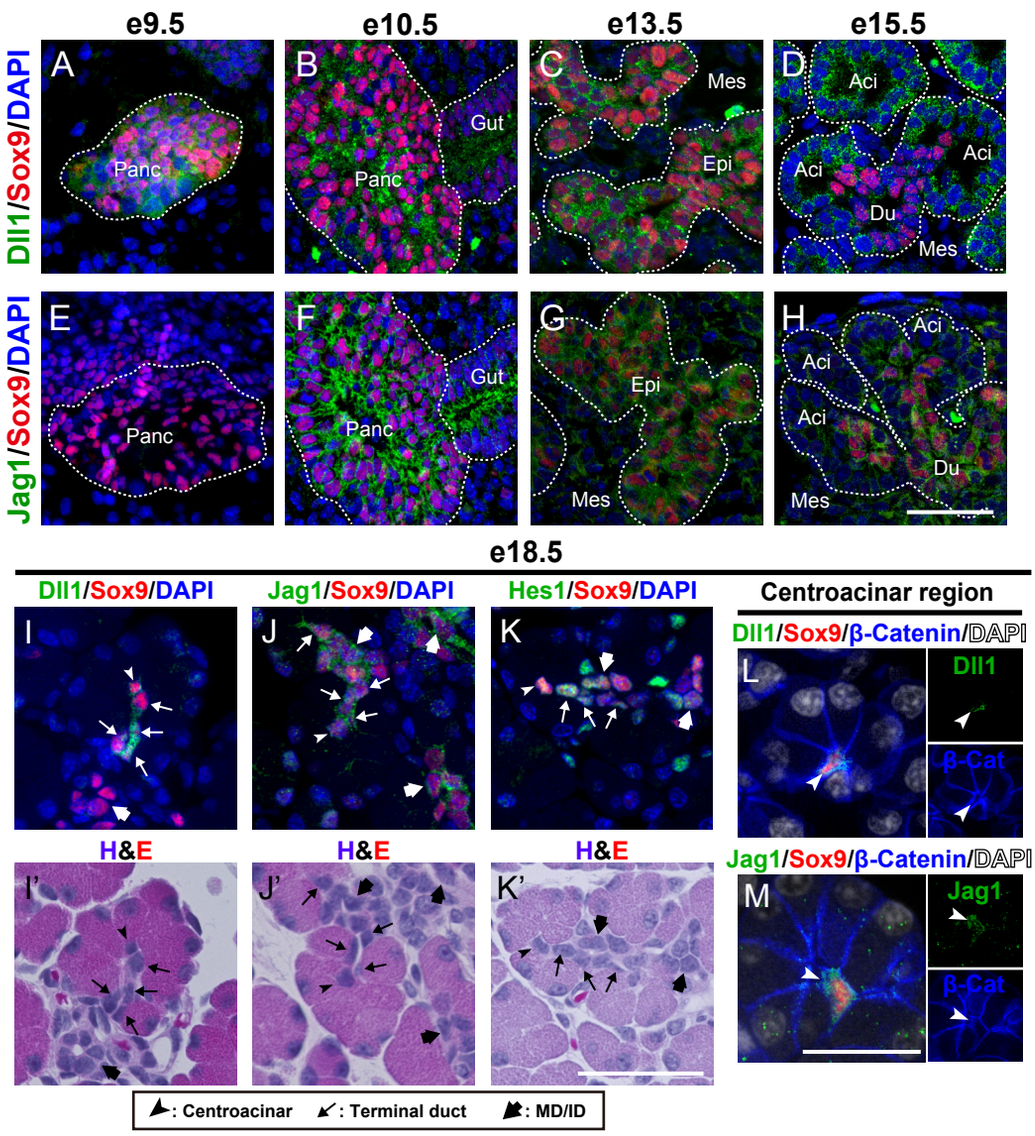
e9.5
e10.5
e13.5
e15.5
Dll1/Sox9/DAPI
Jag1/Sox9/DAPI
A
B
C
D
E
F
G
H
Panc
Gut
Mes
Epi
Aci
Du
e18.5
Dll1/Sox9/DAPI
Jag1/Sox9/DAPI
Hes1/Sox9/DAPI
Centroacinar region
Dll1/Sox9/β-Catenin/DAPI
Jag1/Sox9/β-Catenin/DAPI
I
J
K
L
M
Dll1
Jag1
β-Cat
H&E
I'
J'
K'
: Centroacinar
: Terminal duct
: MD/ID

Nakano Fig.2

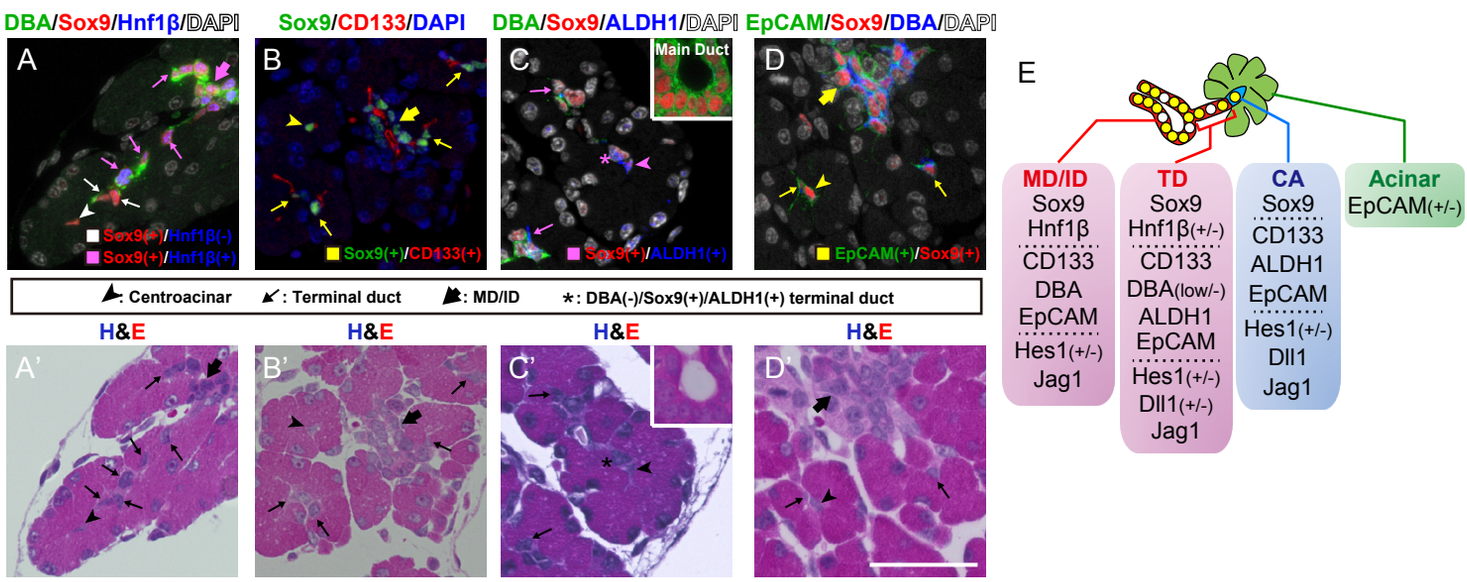
DBA/Sox9/Hnf1β/DAPI
Sox9/CD133/DAPI
DBA/Sox9/ALDH1/DAPI
EpCAM/Sox9/DBA/DAPI
A
B
C
D
Main Duct
Sox9(+)/Hnf1β(-)
Sox9(+)/Hnf1β(+)
Sox9(+)/CD133(+)
Sox9(+)/ALDH1(+)
EpCAM(+)/Sox9(+)
: Centroacinar
: Terminal duct
: MD/ID
*: DBA(-)/Sox9(+)/ALDH1(+) terminal duct
H&E
H&E
H&E
H&E
A'
B'
C'
D'
E
MD/ID
Sox9
Hnf1β
CD133
DBA
EpCAM
Hes1(+/-)
Jag1
TD
Sox9
Hnf1β(+/-)
CD133
DBA(low/-)
ALDH1
EpCAM
Hes1(+/-)
Dll1(+/-)
Jag1
CA
Sox9
CD133
ALDH1
EpCAM
Hes1(+/-)
Dll1
Jag1
Acinar
EpCAM(+/-)

Nakano Fig.3

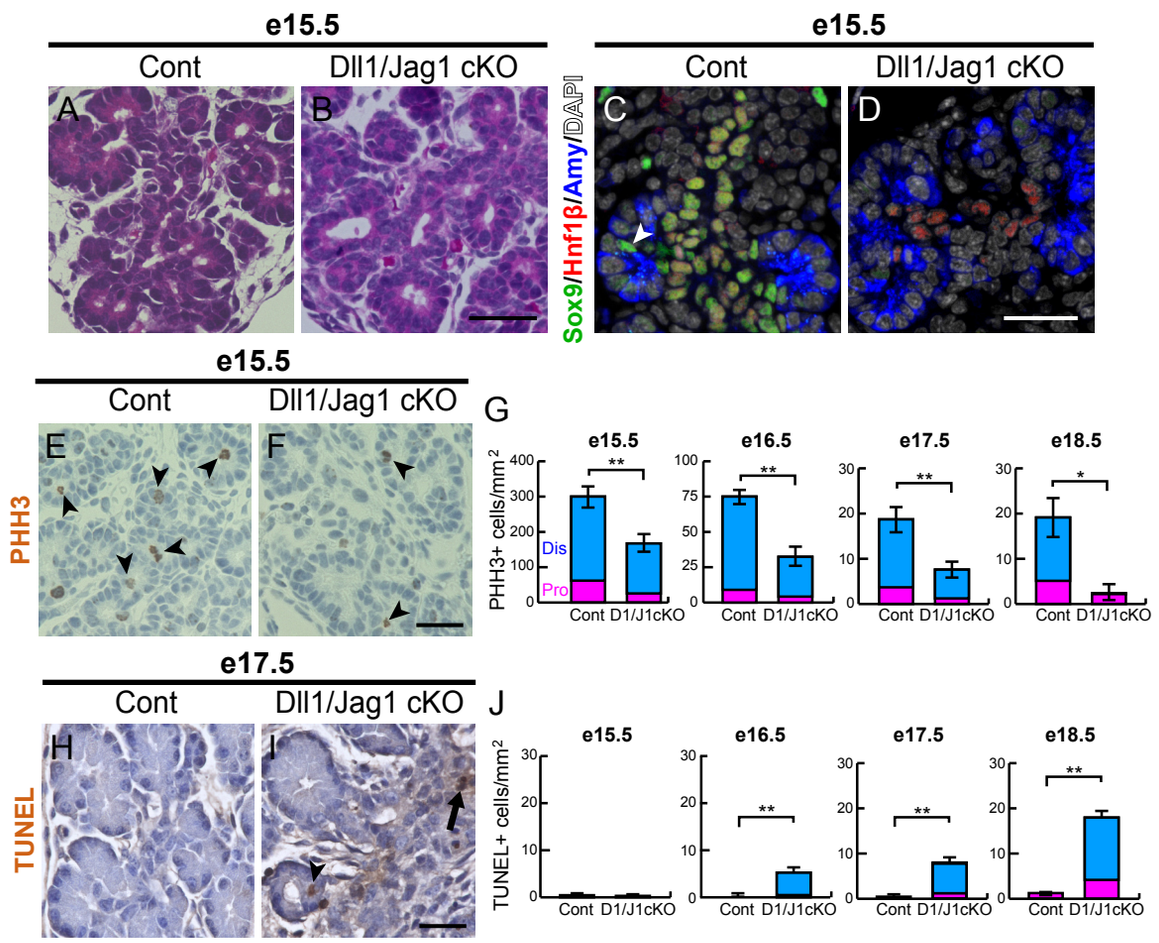
e15.5
Cont
Dll1/Jag1 cKO
A
B
e15.5
Cont
Dll1/Jag1 cKO
C
D
Sox9/Hnf1β/Amy/DAPI
e15.5
Cont
Dll1/Jag1 cKO
PHH3
E
F
G
e15.5
e16.5
e17.5
e18.5
PHH3+ cells/mm2
Dis
Pro
Cont D1/J1cKO
e17.5
Cont
Dll1/Jag1 cKO
TUNEL
H
I
J
e15.5
e16.5
e17.5
e18.5
TUNEL+ cells/mm2
Cont D1/J1cKO

Nakano Fig.4

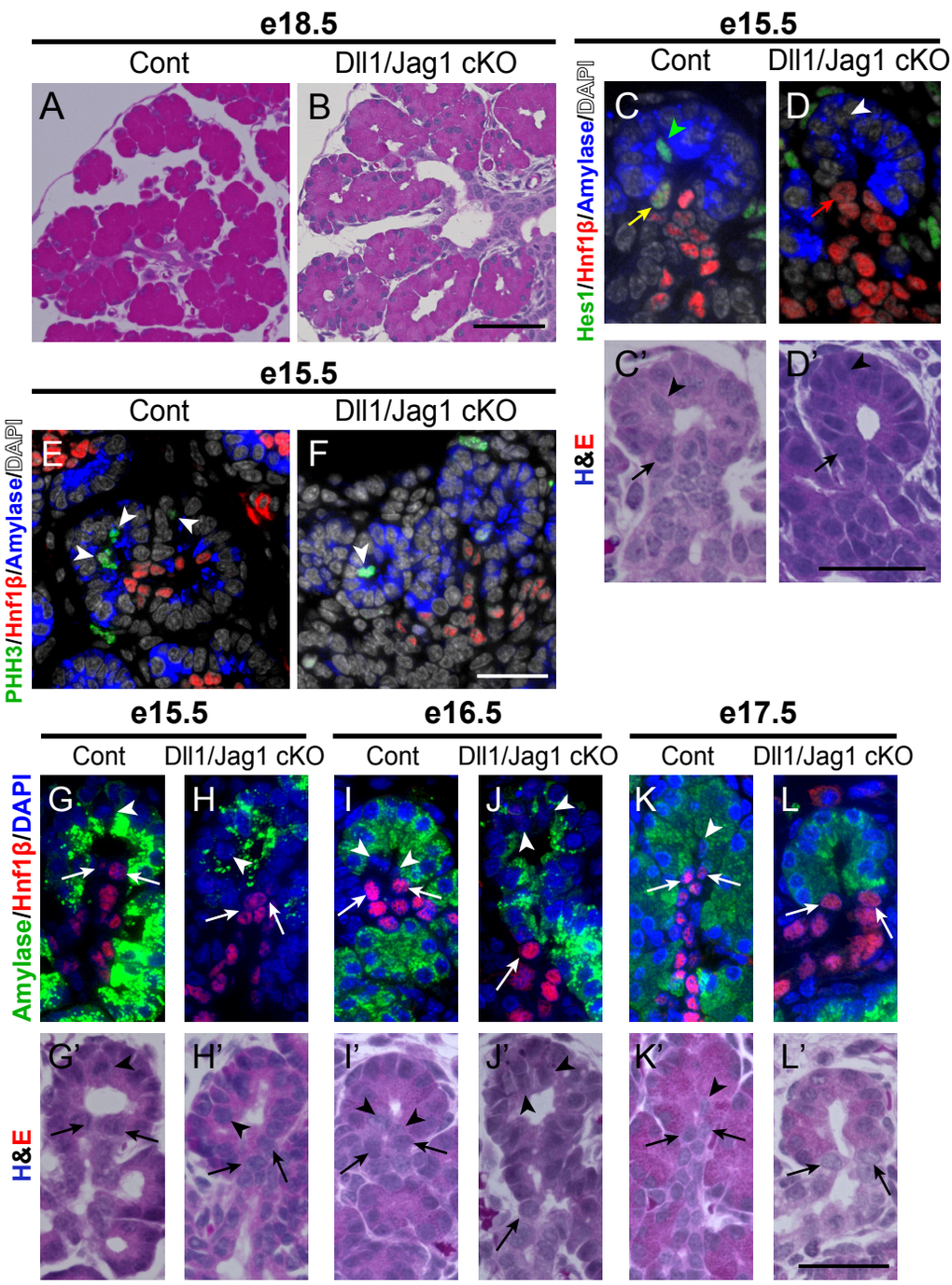
e18.5
Cont
Dll1/Jag1 cKO
A
B
e15.5
Cont
Dll1/Jag1 cKO
Hes1/Hnf1β/Amylase/DAPI
C
D
C'
D'
H&E
e15.5
Cont
Dll1/Jag1 cKO
PHH3/Hnf1β/Amylase/DAPI
E
F
e15.5
e16.5
e17.5
Cont
Dll1/Jag1 cKO
Amylase/Hnf1β/DAPI
G
H
I
J
K
L
H&E
G'
H'
I'
J'
K'
L'

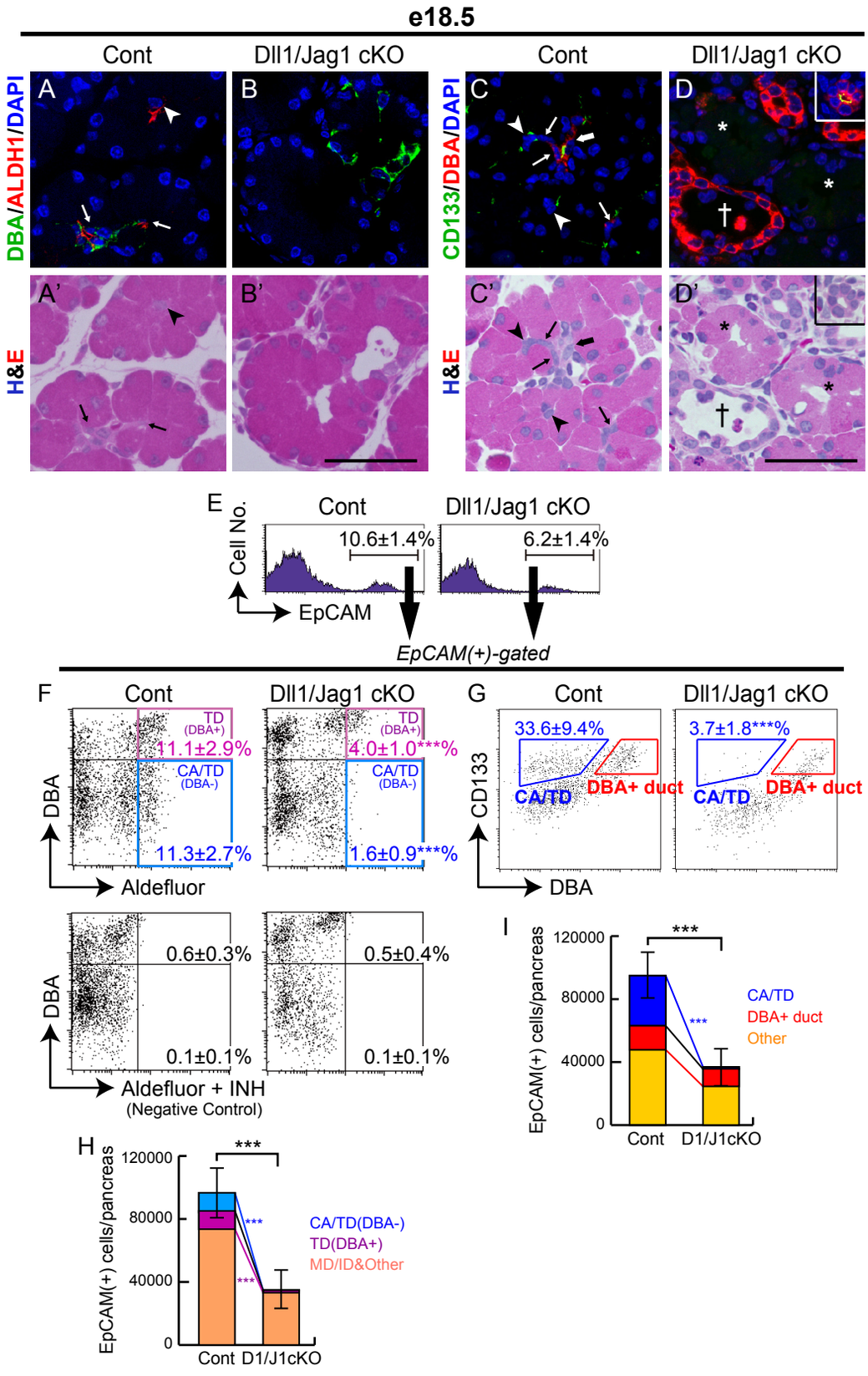
e18.5
Cont
Dll1/Jag1 cKO
Cont
Dll1/Jag1 cKO
DBA/ALDH1/DAPI
CD133/DBA/DAPI
H&E
H&E
A
B
C
D
A'
B'
C'
D'
E
Cell No.
Cont
Dll1/Jag1 cKO
10.6±1.4%
6.2±1.4%
EpCAM
EpCAM(+)-gated
F
Cont
Dll1/Jag1 cKO
TD (DBA+)
11.1±2.9%
4.0±1.0***%
CA/TD (DBA-)
11.3±2.7%
1.6±0.9***%
DBA
Aldefluor
0.6±0.3%
0.5±0.4%
0.1±0.1%
0.1±0.1%
DBA
Aldefluor + INH
(Negative Control)
G
Cont
Dll1/Jag1 cKO
33.6±9.4%
3.7±1.8***%
CA/TD
DBA+ duct
CA/TD
DBA+ duct
CD133
DBA
I
***
120000
80000
40000
0
***
CA/TD
DBA+ duct
Other
EpCAM(+) cells/pancreas
Cont
D1/J1cKO
H
***
120000
80000
40000
0
***
***
CA/TD(DBA-)
TD(DBA+)
MD/ID&Other
EpCAM(+) cells/pancreas
Cont
D1/J1cKO